Remote Sensing of Environment 131 (2013) 275–286

Contents lists available at SciVerse ScienceDirect

Remote Sensing of Environment

journal homepage: www.elsevier.com/locate/rse

Evaluation of MODIS gross primary productivity for Africa using eddy covariance data

M. Sjöström [a], M. Zhao [b], S. Archibald [c], A. Arneth [d], B. Cappelaere [e], U. Falk [f], A. de Grandcourt [g,h], N. Hanan [i], L. Kergoat [j], W. Kutsch [k], L. Merbold [l], E. Mougin [j], A. Nickless [c], Y. Nouvellon [g,h,m], R.J. Scholes [c], E.M. Veenendaal [n], J. Ardö [a,*]

[a] Department of Physical Geography and Ecosystem Science, Lund University, Sölvegatan 12, 22362, Lund, Sweden
[b] Department of Geographical Sciences, University of Maryland, College Park, MD 20740, USA
[c] CSIR Natural Resources and Environment, P.O. Box 395, Pretoria 0001, South Africa
[d] Karlsruhe Institute of Technology, Institute of Meteorology and Climate Research/Atmospheric Environmental Research, 82467, Garmisch-Partenkirchen, Germany
[e] IRD, HydroSciences, BP 64501, 34394 Montpellier Cedex 5, France
[f] Center for Remote Sensing of Land Surfaces, University of Bonn, Bonn, Germany
[g] CIRAD, UMR 111, Ecologie Fonctionnelle & Biogéochimie des Sols & Agro-écosystèmes, F-34060 Montpellier, France
[h] CRDPI, BP 1291, Pointe-Noire, Republic of the Congo
[i] Geographic Information Science Center of Excellence (GIScCE), South Dakota State University, Brookings, SD 57007, USA
[j] GET, University of Toulouse 3, CNRS, IRD, UMR 5563, F-31400 Toulouse, France
[k] Thünen Institue for Climate-Smart Agriculture, Bundesalle 50, 38116 Braunschweig, Germany
[l] ETH Zurich, Department of Environmental Systems Science, Institute of Agricultural Sciences, Universitätsstrasse 2, 8092 Zurich, Switzerland
[m] USP, Universidade de São Paulo, ESALQ, Departamento de Ciências Atmosféricas, IAG, CEP 05508-900 São Paulo, Brazil
[n] Nature Conservation and Plant Ecology Group, Wageningen University, Droevendaalsesteeg 3a, 6700 AA Wageningen, The Netherlands

ARTICLE INFO

Article history:
Received 3 January 2012
Received in revised form 19 November 2012
Accepted 21 December 2012
Available online 28 January 2013

Keywords:
Remote sensing
Africa
Gross primary production (GPP)
Moderate Resolution Imaging Spectroradiometer (MODIS)
MOD17A2
CarboAfrica
AMMA

ABSTRACT

MOD17A2 provides operational gross primary production (GPP) data globally at 1 km spatial resolution and 8-day temporal resolution. MOD17A2 estimates GPP according to the light use efficiency (LUE) concept assuming a fixed maximum rate of carbon assimilation per unit photosynthetically active radiation absorbed by the vegetation (ε_{max}). Minimum temperature and vapor pressure deficit derived from meteorological data down-regulate ε_{max} and constrain carbon assimilation. This data is useful for regional to global studies of the terrestrial carbon budget, climate change and natural resources. In this study we evaluated the MOD17A2 product and its driver data by using in situ measurements of meteorology and eddy covariance GPP for 12 African sites. MOD17A2 agreed well with eddy covariance GPP for wet sites. Overall, seasonality was well captured but MOD17A2 GPP was underestimated for the dry sites located in the Sahel region. Replacing the meteorological driver data derived from coarse resolution reanalysis data with tower measurements reduced MOD17A2 GPP uncertainties, however, the underestimations at the dry sites persisted. Inferred ε_{max} calculated from tower data was higher than the ε_{max} prescribed in MOD17A2. This, in addition to uncertainties in fraction of absorbed photosynthetically active radiation (FAPAR) explains some of the underestimations. The results suggest that improved quality of driver data, but primarily a readjustment of the parameters in the biome parameter look-up table (BPLUT) may be needed to better estimate GPP for African ecosystems in MOD17A2.

1. Introduction

Rising levels of atmospheric concentrations of CO_2 and other greenhouse gases have increased the global average air temperature and higher temperatures are predicted to influence future patterns and magnitudes of precipitation (Solomon et al., 2007). Taken together, the changing temperature, precipitation and atmospheric CO_2 burdens are likely to cause shifts in terrestrial productivity. This may in turn crucially influence the availability of biomass resources like timber or crop and pasture yields. The IPCC (Intergovernmental Panel on Climate Change) reports that by 2020 between 75 and 200 million Africans will suffer from increased water stress (Parry et al., 2007), and in some African countries, the yield from rain-fed agriculture could be decreased (Schlenker & Lobell, 2010). So far, a small amount of scientific data and literature exist on the carbon cycle and climate variability and trends in Africa (Hulme et al., 2001; Merbold et al., 2009; Nicholson, 2000, 2001; Williams et al., 2008, 2007) compared to North America, Europe and Asia owing to

* Corresponding author at: Department of Physical Geography and Ecosystem Science, Lund, Sweden. Tel.: +46 462224031; fax: +46 462224011.
E-mail address: jonas.ardo@nateko.lu.se (J. Ardö).

0034-4257/$ – see front matter © 2013 Elsevier Inc. All rights reserved.
http://dx.doi.org/10.1016/j.rse.2012.12.023

the sparse network of climate stations, eddy covariance stations, and long term ecological research sites. Consequently, our understanding of responses of vegetation productivity and the carbon cycle to climate variability in African ecosystems is poor which severely limits assessments of ecosystem vulnerability and adaptation potentials.

In 2006, CarboAfrica was established with the purpose of providing increased knowledge of Africa's role in the global carbon cycle (Bombelli et al., 2009). The project's objectives included a synthesis of flux data from existing eddy covariance sites in Africa, as well as to support new observations. The eddy covariance technique (e.g. Aubinet et al., 2000; Baldocchi et al., 2001; Lindroth, Grelle, & Moren, 1998; Wofsy et al., 1993) has become a standard for measuring fluxes of carbon, water and energy between the land and atmosphere at the ecosystem scale and provides an excellent opportunity for validation of model estimates of carbon flux from terrestrial ecosystems.

Gross primary production (GPP) is the capacity of the vegetation to capture carbon and energy during photosynthesis. GPP can be derived from eddy covariance measurements through estimates of net ecosystem exchange (NEE) and ecosystem respiration (R_{eco}). The Net primary productivity (NPP) is the net carbon stored after subtracting the autotrophic plant respiration from GPP. While some of the annual NPP in an ecosystem may also be lost by episodic events like windthrow or fire, it is the basis for essential ecosystem services such as fuel, food, feed, fiber and material for construction purposes (Richmond, Kaufmann, & Myneni, 2007). As access to these resources and services is crucial, monitoring of primary productivity is important in assessing the variability of resources and in evaluating the impact of climate change on plant production (e.g. Schwalm, Williams, & Schaefer, 2011; Zhao & Running, 2010).

The Moderate Resolution Imaging Spectroradiometer (MODIS) on board the TERRA and AQUA satellites provides data at high spatial and temporal resolution free of cost. MOD17 is the standard product on primary production and is derived partly from MODIS data. The product uses the light use efficiency (LUE) concept developed by Monteith (1977); Montieth (1972) where GPP is a function of the absorbed photosynthetically active radiation (APAR) by plants and the conversion efficiency of absorbed light energy (ε). MOD17 GPP data are available across the globe at an 8-day temporal resolution and a 1×1 km spatial resolution from 2000 in close to real time (one to two weeks delay) (Heinsch et al., 2003).

Since MOD17 is the first continuously available satellite data driven primary production dataset it has undergone several validation studies. As part of the BigFoot project, Turner et al. (2005) evaluated the MODIS GPP product (collection 4.5) across 6 sites in North America by implementing a scaling approach that relied on the Biome-BGC (BioGeochemical Cycles) model with inputs of ground measurements and Landsat ETM+ imagery (Turner et al., 2003). A good agreement between ground-based GPP and MODIS GPP was found for a coniferous forest site with an underestimation at an agricultural site and overestimation at an Arctic tundra and at a desert grassland site. Under- and over-predictions of MODIS GPP were concluded to be mainly attributed to inaccuracies in the parameterization of maximum light use efficiency (ε_{max}) and in the seasonality of MODIS derived fraction of absorbed photosynthetically active radiation (FAPAR, collection 4). Heinsch et al. (2006) carried out a comprehensive evaluation of MOD17 (collection 4.5) comparing MODIS GPP derived with both DAO (NASA'S Data Assimilation Office) meteorology and tower-specific meteorology to eddy covariance based GPP data across 15 sites in North America. The authors found that MODIS GPP with DAO meteorology overestimated annual GPP whereas use of local tower-meteorology in the MODIS GPP algorithm led to an underestimation across sites. Heinsch et al. (2006) further suggested problems with the algorithm at a water limited site, which has also been noted by a number of other authors (Coops et al., 2007; Kanniah et al., 2009; Leuning et al., 2005). Leuning et al. (2005) evaluated MODIS GPP (collection 4.0) against eddy covariance GPP from a tropical savanna site and a Eucalyptus forest site in Australia and noted quite large discrepancies at both sites. The authors managed to improve MODIS GPP predictions by introducing an additional soil water parameter to the algorithm. Using soil moisture rather than atmospheric vapor pressure deficit (VPD) to reduce ε_{max} as a result of limited water availability was also suggested by Coops et al. (2007), who evaluated MODIS GPP (collection 4.5) coupled with 8-day tower meteorology at a needle leaf forest site in North America. The authors observed a strong correlation between eddy covariance GPP and predictions of GPP by the MODIS algorithm, but with an underestimation of 30%. Implementing the same soil water modifier as proposed by Leuning et al. (2005) in the MODIS GPP algorithm yielded a slightly improved correlation and Coops et al. (2007) attributed the underestimation observed between measured and modeled GPP to the level of MODIS ε_{max}. Kanniah et al. (2009) evaluated MODIS GPP (collections 4.5, 4.8 and 5.0) using both DAO and tower meteorology as inputs to the algorithm at a tropical woody savanna site in northern Australia. The authors noted a negative bias in GPP due to ε_{max} and VPD in collection 5.0 and recommended a readjustment of these parameters in the algorithm to achieve a more accurate estimation of GPP at the site. Kanniah et al. (2009) also observed improved capture of seasonal GPP dynamics when the VPD-scalar was replaced by the Evaporative Fraction (the ratio of the energy exported as evaporated water to the total amount of energy, EF).

Although a number of studies over tropical dryland ecosystems have helped to increase confidence in the MODIS products (Fensholt, Sandholt, & Rasmussen, 2004; Fensholt et al., 2006; Huemmrich et al., 2005; Kanniah et al., 2009; Leuning et al., 2005), few have evaluated the MODIS primary production algorithm for ecosystems in Africa. Fensholt et al. (2006) compared field measured above ground NPP in semi-arid Senegal against MODIS net photosynthesis (PsnNet, collection 4.0) and MODIS annual NPP (collections 4.0 and 4.5). The authors observed moderate relationships and found that MODIS underpredicted NPP in this region due to the biome parameter look-up table (BPLUT) values controlling the maintenance respiratory costs by leaves and roots. Sjöström et al. (2011) found that MODIS GPP (collection 5) performed reasonably well in explaining the variability in eddy covariance GPP at a range of African ecosystems. However, the product was observed to underestimate GPP across sites, most significantly in dry savanna ecosystems in the Sahel.

Even though the coarse spatial resolution of the reanalysis meteorology data can introduce uncertainties in MODIS GPP at certain sites (Zhao, Running, & Nemani, 2006), there is a general agreement that performance of the MODIS GPP product in predicting GPP is good across a range of climates under normal conditions (Plummer, 2006). Studies that have utilized a ground-based GPP scaling approach or that have coupled MODIS GPP with tower meteorology to evaluate the algorithm have noted that there is a potential for improvements (Heinsch et al., 2006; Kanniah et al., 2009; Turner et al., 2003, 2005), some of which have already been made (Zhao et al., 2005). However, gaps still exist in the representation of biomes as there is, in general, a rather strong focus on northern latitude ecosystems. Syntheses of eddy covariance data through networks such as CarboAfrica or AMMA (African Monsoon Multidisciplinary Analyses) (Lebel et al., 2009) are critical to reduce this bias and to ensure continuous evaluation of satellite based biophysical products.

This paper evaluates the MODIS GPP product using eddy covariance data from 12 sites in Africa (Table 1, Fig. 1). The objectives of this paper are: to evaluate the MOD17A2 GPP product for Africa through comparisons with GPP estimated from eddy covariance and; to evaluate the role and uncertainty of the variables (meteorological data derived from coarse resolution reanalysis, ε_{max} and FAPAR) used in the algorithm.

Table 1
Site descriptions including name (abbreviation), latitude and longitude (lat/long, decimal degrees), general ecosystem type, dominant MOD12Q1 land cover class (5×5 km window), mean annual long-term precipitation (MAP, mm), mean annual temperature (MAT, °C), years of measurements, number of weekly GPP data points and references.

Name	Lat	Lon	Ecosystem	(MOD12Q1 Cover)	MAP (mm)	MAT (°C)	Years with data	Weeks with data	References
Bontioli (BF-BON)	10.87	−3.07	Grassland/shrubland	Savanna	926	26.1	2004, 2006	43	Brummer et al. (2008)
Maun (BW-MA1)	−19.92	23.56	Woodland	Savanna	465	22.0	1999–2001	93	Veenendaal, Kolle, and Lloyd (2004)
Hinda (CG-HIN)	−4.68	12.00	Forest	Savanna	1200	23.7	2001–2002	71	Longdoz et al. (2010)
Tchizalamou (CG-TCH)	−4.29	11.66	Grassland	Savanna	1150	26.0	2006–2007	70	Merbold et al. (2009)
Agoufou (ML-AGG)	15.34	−1.48	Open woody savanna	Grassland	374	30.2	2007–2008	34	Timouk et al. (2009)
Kelma (ML-KEM)	15.22	−1.57	Open forest (seasonally flooded)	Grassland	374	30.2	2007–2008	76	Timouk et al. (2009)
Wankama Fallow (NE-WAF)	13.65	2.63	Shrubland	Grassland	510	29.5	2005–2006	78	Ramier et al. (2009)
Wankama Millet (NE-WAM)	13.64	2.63	Cropland	Grassland	510	29.5	2005–2006	72	Boulain et al. (2009)
Demokeya (SD-DEM)	13.28	30.48	Grassland/savanna	Open shrubland	320	26.0	2007–2009	109	Ardö et al. (2008)
Skukuza (ZA-KRU)	−25.02	31.50	Wooded grassland	Savanna	545	22.0	2000–2008	339	Kutsch et al. (2008)
Malopeni (ZA-MAP)	−23.83	31.21	Savanna	Savanna	458	22.2	2009	41	–
Mongu (ZM-MON)	−15.44	23.25	Woodland	Savanna	945	24.5	2007–2009	90	Merbold et al. (2009)

2. Data and methodology

2.1. The MOD17 algorithm

MOD17 consist of two products, MOD17A2 and MOD17A3. MOD17A2 contains both 8-day GPP and 8-day PSNnet, whereas MOD17A3 contains annual sums of NPP (Heinsch et al., 2003). APAR is calculated as the product of incoming photosynthetically active radiation (PAR) and FAPAR whereas GPP is calculated as:

$$GPP = PAR \times FAPAR \times \varepsilon \tag{1}$$

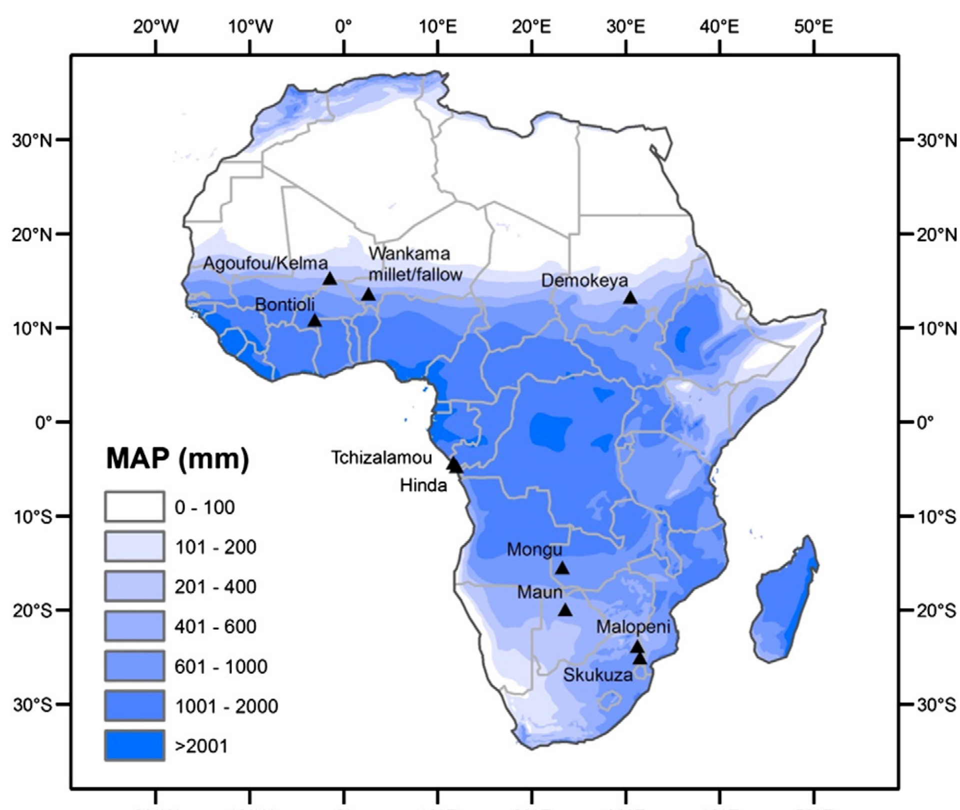

Fig. 1. Mean annual precipitation (MAP, mm) across Africa and locations of eddy covariance sites included in this study (rainfall data from UNEP/GRID, grid.unep.ch/).

where PAR is determined as a fraction of the incident shortwave radiation ($S_{\downarrow}$)

$$PAR = S_{\downarrow} \times 0.45 \tag{2}$$

and ε is calculated by modifying ε_{max} by scalars of daily VPD (VPD_s) and low daily minimum air temperature (T_s) that reduce ε_{max} at cold temperatures and/or high VPD:

$$\varepsilon = \varepsilon_{max} \times T_s \times VPD_s. \tag{3}$$

The MODIS GPP 5.1 data used in this paper implements 6-hourly National Center for Environmental Prediction-Department of Energy (NCEP-DOE) reanalysis II data for air temperature, VPD and $S_{\downarrow}$. In MODIS GPP 5.1 the original NCEP-DOE reanalysis II data is interpolated from the original resolution of approximately 1.9° latitude × 1.9° longitude to 1 × 1 km grids according to Zhao et al. (2005). FAPAR in the MODIS GPP algorithm is derived from the 8-day MOD15A2 1 km product, and the 1 km University of Maryland (UMD) land cover classification scheme in the MOD12Q1 product is used to map biome specific physiological parameters (ε_{max}, minimum and maximum temperature and VPD) using a BPLUT.

For each site we extracted the MOD12Q1 land cover data (UMD), NCEP-DOE reanalysis II data and 8-day MOD17A2 GPP. This was done for the period from 2000 to 2009 for the 1 × 1 km tower pixels (Connolly et al., 2009; Zhang et al., 2006) and the 5 × 5 km area centered over each of the flux towers.

2.2. Data from the flux towers

2.2.1. Eddy covariance and meteorological data

Twelve eddy covariance measurement sites associated with CarboAfrica and AMMA were used and represent a variety of African ecosystems and rainfall regimes (Fig. 1, Table 1). The sites cover a diversity of climate and vegetation types with five sites in the Sahel (Wankama Millet, Wankama fallow, Kelma, Agoufou and Demokeya), one in the Sudanian zone (Bontioli), two in the more humid region close to the equator (Tchizalamou and Hinda) and four sites in the semi-arid and sub humid regions of southern Africa (Maun, Mongu, Skukuza and Malopeni).

Eddy covariance data were either collected from participating site researchers or downloaded directly from the CarboAfrica network website (gaia.agraria.unitus.it/home/sites-list). For all sites, except Wankama Millet and Fallow, the gap-filled and flux-partitioned Level 4 CarboAfrica product was used (Papale et al., 2006; Reichstein et al., 2005). This product contains a number of gap-filled meteorological and environmental variables, including GPP calculated from NEE. In the Level 4 CarboAfrica product NEE is either estimated through the storage correction obtained by applying the discrete approach (same for all sites) or by using the storage correction determined by the principal investigator at each site. NEE is then gap-filled using the Marginal Distribution Sampling (MDS) method (Reichstein et al., 2005) or the Artificial Neural Network (ANN) method (Papale & Valentini, 2003). For sites for which the Level 4 CarboAfrica product was available we used standardized GPP data calculated from NEE filled using the MDS approach, whereas GPP from Wankama millet and fallow was derived from NEE gap-filled according to the MDS approach by using publicly available methods at bgc-jena.mpg.de/bgc-mdi/html/eddyproc/index.html (Reichstein et al., 2005). Collected flux data originate from year 2000 up to 2009 with only a few years of data available for most sites (Table 1).

Meteorological data (PAR, air temperature and VPD) measured at the flux towers (here forth referred to as tower data) originated from the same sources as described above for the eddy covariance data. These tower data were directly compared to the NCEP-DOE reanalysis II data to assess how well the reanalysis data set represented the local conditions. Details on the instrumentation and other characteristics at each site are available from the references listed in Table 1. Furthermore, the tower data was used as input to the MOD17A2 algorithm to compare GPP estimated using the tower data with the NCEP-DOE reanalysis II data.

2.2.2. FAPAR, data uncertainty and light use efficiency

To study the influence of FAPAR on GPP we replaced the FAPAR used in the MOD17 GPP calculation with field calculated FAPAR for one site-year (SD-DEM, 2009). Red (center bandwidth: 655 nm) and NIR (center bandwidth: 855 nm) in situ measured reflectance were averaged from 0900 to 1500 (Fensholt et al., 2004). In situ FAPAR was then calculated through use of the simple ratio (SR) using the formulations by Sellers et al. (1996):

$$FAPAR = \frac{(SR - SR_{\min}) \times (FAPAR_{\max} - FAPAR_{\min})}{SR_{\max} - SR_{\min}} + FAPAR_{\min}, \tag{4}$$

where SR is the simple ratio (NIR/Red reflectance), $FAPAR_{max}$ and $FAPAR_{min}$ were assumed to be 0.9 and 0.01 respectively whereas the vegetation cover dependent values of SR_{min} and SR_{max}, derived from Advanced Very High Resolution Radiometer data, were set to 1.81 and 5.35 (Sellers et al., 1996).

In order to estimate the propagation of uncertainty from VPD, incoming PAR and FAPAR to annual GPP we used Monte Carlo analysis. The RMSE's derived from the comparisons of NCEP/DOE II and of MOD17A2 FAPAR with tower data for SD-DEM (PAR: 2.8 MJ, VPD: 1196 Pa, FAPAR: 0.8) were used to represent the standard deviations assuming normal distribution for all variables (T_{min} was not included as daytime temperatures were rarely less than 12.0 °C). For each variable 500 simulations were performed, as well as 500 simulations where all three variables were varied randomly and independently

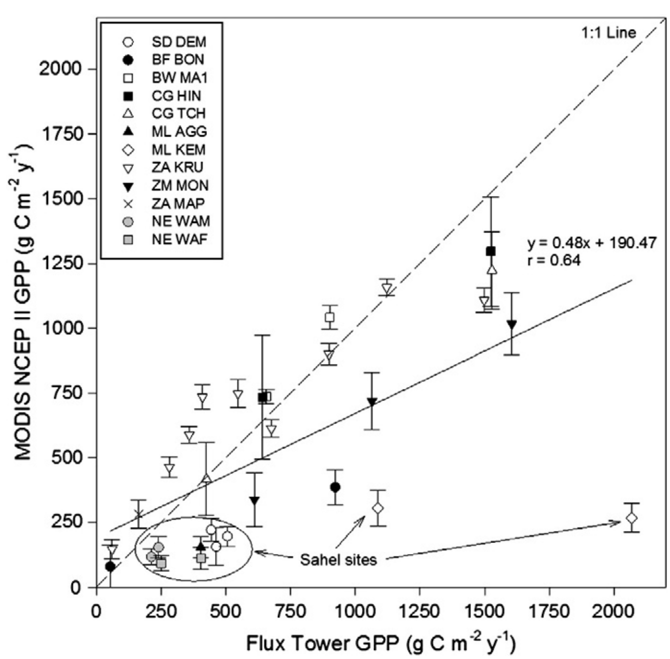

Fig. 2. Annual sums of eddy covariance estimated GPP (g C m^{-2} $year^{-1}$) versus MOD17A2 NCEP II GPP (g C m^{-2} $year^{-1}$). Bars represents standard deviation of MOD17A2 GPP sums over the 5 × 5 pixels centered on the eddy covariance tower. Data for all sites included when both eddy covariance and MOD17A2 NCEP II GPP were available (see Table 2 for the number of available observations per year).

allowing an estimate of the combined data uncertainty on annual GPP.

3. Results

3.1. MOD17A2 NCEP II GPP validation

MOD17A2 NCEP II GPP was compared to eddy covariance GPP and results are shown in Figs. 2, 3 and 4A. Fig. 2 shows yearly sums of GPP measured by eddy covariance versus sums of GPP from MOD17A2 NCEP II based on the amount of available observations per year (Table 2). Fig. 3 illustrates time-series of MOD17A2 NCEP II GPP and eddy covariance GPP and Fig. 4A shows a scatterplot between 8-day eddy covariance GPP against 8-day MOD17A2 NCEP II GPP.

A modest correlation was found between MOD17A2 NCEP II GPP and eddy covariance derived GPP for all sites and observations ($r=0.57$, RMSE = 2.58 g C m^{-2} day^{-1}, Fig. 4A). Substantial variations existed between sites and between years ($r=0.24$ to 0.92, RMSE = 0.66 to 8.09 g C m^{-2} day^{-1}, Table 2). As can be seen in Figs. 2 and 3 and in Table 2 MOD17A2 NCEP II underestimates GPP for the majority of site-years. The mean difference for all sites and observations was −0.70 g C m^{-2} day^{-1}. Yearly mean differences between MOD17A2 NCEP II GPP and eddy covariance GPP ranged between an underestimation of −5.80 g C m^{-2} day^{-1} for ML-KEM in 2008, to an overestimation of 1.92 g C m^{-2} day^{-1} for ZA-KRU in 2006 (Table 2). A greater negative mean difference and larger RMSE was observed for the Sahelian sites (−1.72 g C m^{-2} day^{-1}, RMSE = 3.54) when compared to other sites (−0.22 g C m^{-2} day^{-1}, RMSE = 2.03). Excluding data outside the vegetation growing period (defined here when eddy covariance GPP < 1 g C m^{-2} day^{-1}; i.e., during the dry season) generally revealed a decline in r and an increase in RMSE (Table 2). However, decreased, increased as well as unchanged relationships were found within individual site-years. For some site-years the remaining number of observations was too low to yield meaningful correlations when including data from the vegetation season only (e.g. ZA-MAP).

For the majority of sites the seasonality, start and end of the vegetation season were well captured by MOD17A2 NCEP II GPP (Fig. 3). However, significant underestimations were observed at the peak of the vegetation period for most of the sites. One of the possible explanations for the deviations observed between MOD17A2 and eddy

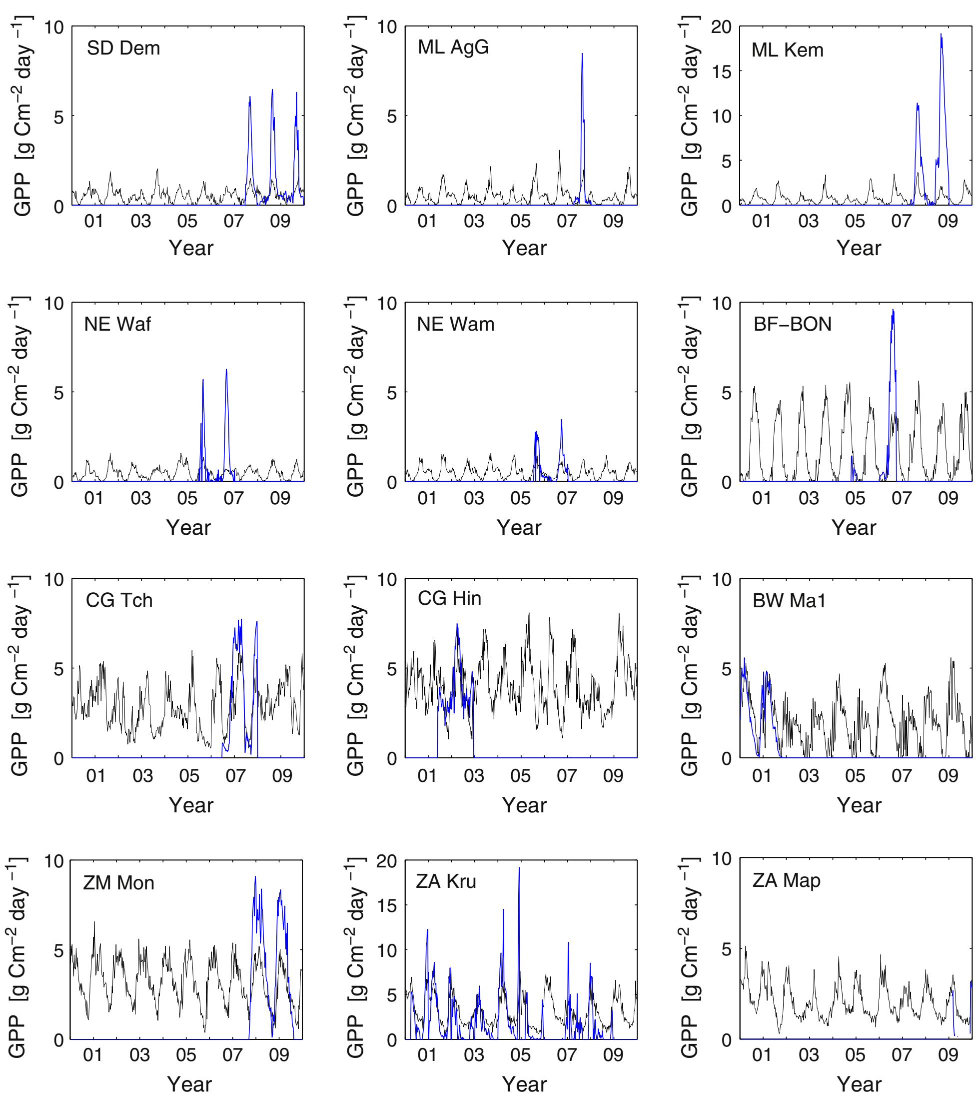

Fig. 3. Time series of 8-day MOD17A2 NCEP II GPP (g C m^{-2} day^{-1}) from 2000 to 2009 (solid black line) and 8-day eddy covariance GPP (g C m^{-2} day^{-1}) (solid blue line). Note that the ranges of y-axis for ML-KEM and ZA-KRU are different than for the other sites.

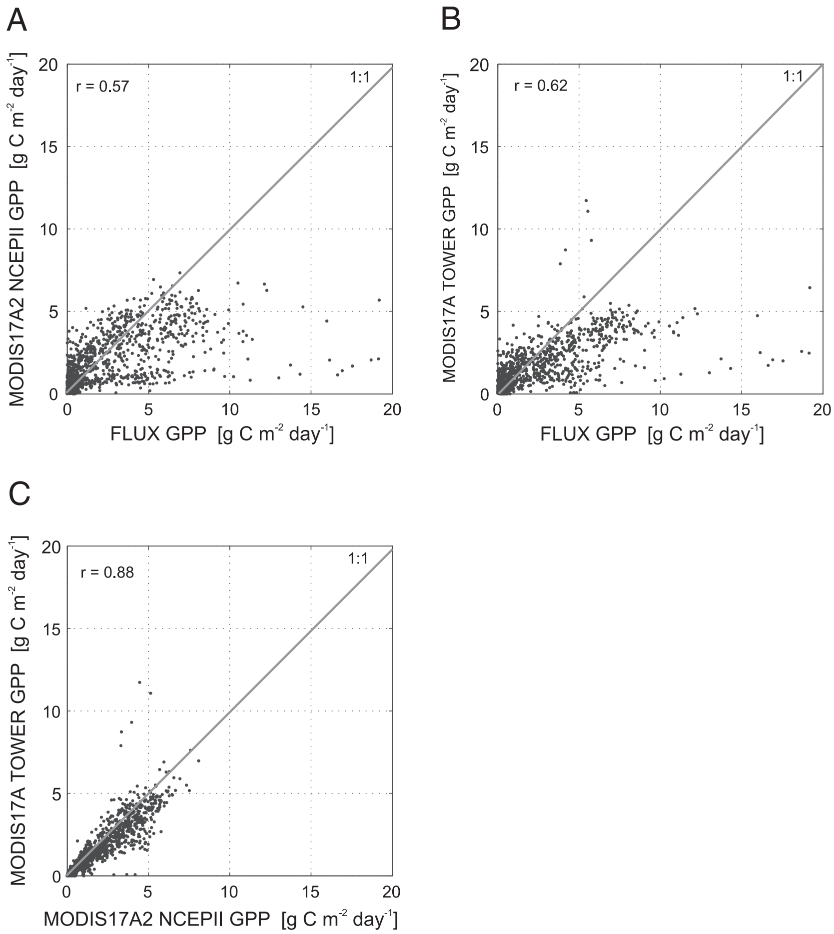

Fig. 4. Scatter plots of 8-day data with MOD17A2 GPP driven with NCEP-DOE II against eddy covariance GPP (A), MOD17A2 GPP driven with tower data against eddy covariance GPP (B) and MOD17A2 GPP driven with NCEP-DOE II data against MOD17A2 GPP driven with tower data (C).

covariance GPP could be inaccuracies in the NCEP-DOE II reanalysis data used in the product.

3.2. Evaluation of impacts of meteorological data and scalars on ε

Replacing NCEP-DOE II with tower data (here forth referred to as MOD17A2 Tower GPP) for estimating MOD17A2 GPP slightly increased the overall correlation with eddy covariance GPP (r = 0.62, RMSE = 2.58 gC m^{-2} day^{-1}, Fig. 4B). Correlations were observed to increase for 26 of the 31 site years (data not shown), but as with MOD17A2 NCEP II GPP substantial variations existed between sites and between years (r = 0.29 to 0.96, RMSE = 0.51 to 8.31). Results further revealed a correlation of r = 0.88 (RMSE = 0.85 gC m^{-2} day^{-1}) between MOD17A2 NCEP II GPP and MOD17A2 Tower GPP which may indicate a reasonable similarity of the driver data (Fig. 4C).

Correlations between the NCEP-DOE II reanalysis data and local tower data were strongest for temperature, slightly weaker for VPD and with the weakest agreement found for incoming PAR (Fig. 5). As can be seen in Fig. 5A, daily average temperature (T_{avg}) from NCEP-DOE II is underestimated across sites with an average difference of 2.35 °C (r = 0.85, RMSE = 3.5 °C). No clear systematic bias was found for daily minimum temperature (T_{min}) (r = 0.85, RMSE = 2.9 °C, Fig. 5B). For the majority of sites included in this study, the T_{min} function was observed not to constrain MOD17A2 GPP much as only 10% of the daily daytime observations were below 12.0 °C which is the threshold at which daily minimum temperature limits ε for grasslands (Zhao & Running, 2010). The corresponding limit for savannas is 11.4 °C. As GPP at many of these sites is mainly driven by water availability (Merbold et al., 2009), VPD rather than low temperature is likely to have a larger effect on the variability of ε in the MOD17A2 GPP algorithm. NCEP-DOE II slightly underestimates daytime VPD with an average difference of 227 Pa (r = 0.86, RMSE = 738 Pa, Fig. 5C). Fig. 6 further shows scatterplots of eddy covariance GPP against tower VPD for all of the sites broadly divided into savannas and grasslands according to "Ecosystem type" in Table 1. For grasslands there was, in general, a systematic decrease in GPP with increasing VPD and GPP was observed never to exceed 1 gC m^{-2} day^{-2} for VPD-values higher than 4500 Pa (Fig. 6B). There were significant variations in linear regression relationships of GPP versus VPD among sites. For the sites located in the moist tropical regions of Congo (CG-HIN and CG-TCH) VPD was observed to be weakly positively correlated with GPP. Remaining sites were found to be negatively correlated with VPD with correlations ranging from r = −0.21 for ZA-KRU to r = −0.88 for BF-BON. Even though the forested Sahelian site in Mali (ML-KEM) followed the expected pattern with a linear decrease in GPP with increasing VPD, it was observed to have high GPP values (>5 gC m^{-2} day^{-1}) when VPD exceeded 3200 Pa (Fig. 6A).

The relationship between incoming PAR from NCEP-DOE II and incoming PAR from the tower data was scattered (Fig. 5D). High cloud cover can cause substantial daily variation which is reflected in the weak correlation (r = 0.46, RMSE = 2.80 MJ day^{-1}).

3.3. FAPAR and data uncertainty

We compared the FAPAR used in MOD17A2, which originates from the MOD15A2 product (Myneni et al., 2002), with in situ

Table 2
Comparison of MOD17 GPP versus GPP from flux towers in Africa divided per site-year. Number of 8-day values per site-year including all data and during the vegetation season (Vs, GPP > 1 gC m^{-2} day^{-1}), correlation (r), RMSE and mean differences (predicted − observed).

Site/year	Number of Samples		Pearson correlation coefficient (r)		RMSE (g Cm^{-2} day^{-1})		Mean difference [g Cm^{-2} day^{-1}]	
	All	Vs	All	Vs	All	Vs	All	Vs
SD-DEM/2007	23	17	0.89	0.90	2.29	2.66	−1.67	−2.22
SD-DEM/2008	42	14	0.87	0.91	1.86	3.20	−0.92	−2.81
SD-DEM/2009	44	10	0.62	−0.04	1.49	3.09	−0.63	−2.84
BF-BON/2004	9	2	0.88	–	0.66	–	0.36	–
BF-BON/2006	33	17	0.92	0.79	3.10	4.30	−2.07	−3.89
BW-MA1/2000	46	34	0.82	0.59	1.02	1.06	0.37	0.24
BW-MA1/2001	35	26	0.78	0.58	1.03	1.07	0.29	0.10
CG-HIN/2001	28	28	0.40	0.40	1.11	1.11	0.43	0.43
CG-HIN/2002	43	43	0.38	0.38	1.74	1.74	−0.66	−0.66
CG-TCH/2006	25	10	0.72	0.04	1.73	2.40	−0.10	−1.64
CG-TCH/2007	45	35	0.86	0.77	1.76	1.92	−0.85	−1.29
ML-AGG/2007	34	8	0.79	0.30	2.23	4.57	−0.91	−4.03
ML-KEM/2007	26	22	0.87	0.84	4.75	5.16	−3.76	−4.41
ML-KEM/2008	39	28	0.80	0.81	8.09	9.55	−5.80	−8.11
ZA-KRU/2000	28	22	0.84	0.81	2.25	2.43	0.01	−0.34
ZA-KRU/2001	42	28	0.90	0.80	1.44	1.57	0.11	−0.34
ZA-KRU/2002	29	19	0.72	0.74	1.76	1.41	1.40	1.02
ZA-KRU/2003	36	21	0.79	0.66	1.22	1.11	0.70	0.29
ZA-KRU/2004	41	32	0.74	0.65	3.71	4.11	−1.19	−1.97
ZA-KRU/2005	30	8	0.88	0.81	1.15	0.86	0.76	−0.33
ZA-KRU/2006	6	5	0.24	−0.52	2.12	2.12	1.92	1.89
ZA-KRU/2007	27	21	0.59	0.60	2.39	2.50	−0.28	−0.83
ZA-KRU/2008	24	11	0.66	0.41	2.02	2.07	1.20	0.45
ZM-MON/2007	14	13	0.88	0.86	3.19	3.30	−2.56	−2.85
ZM-MON/2008	46	42	0.85	0.83	2.23	2.31	−1.62	−1.84
ZM-MON/2009	28	25	0.90	0.88	2.35	2.45	−1.54	−1.88
ZA-MAP/2009	13	7	0.45	−0.50	1.58	0.63	1.14	0.31
NE-WAM/2005	20	10	0.71	0.35	0.97	1.35	−0.59	−1.29
NE-WAM/2006	35	11	0.80	0.55	0.73	1.25	−0.32	−1.08
NE-WAF/2005	16	9	0.89	0.82	2.00	2.64	−1.23	−2.29
NE-WAF/2006	34	11	0.61	0.53	2.12	3.71	−1.07	−3.33
Min	6	2	0.24	−0.52	0.66	0.63	−5.80	−8.11
Max	46	43	0.92	0.91	8.09	9.55	1.92	1.89

derived FAPAR from 2009 at SD-DEM (Fig. 7A). MODIS GPP uses a linear fitting to fill unreliable MOD15A2 FAPAR (Zhao et al., 2005). Even though the correlation increased by replacing the FAPAR used in MOD17A2 Tower GPP with field calculated FAPAR (r = 0.96, RMSE = 1.28 gC m^{-2} day^{-1}, n = 46) the large underestimation previously observed between MOD17A2 GPP and eddy covariance GPP during the peak vegetation season still persisted for this site (Fig. 7B). In situ calculated FAPAR was in general lower than the MOD17A2 FAPAR during the dry season, however, Fig. 7A mainly reveals that FAPAR in MOD17A2 fails to capture the green-up that occurred in 2009.

The Monte Carlo simulation, based on data from SD-DEM, further revealed that MOD17A2 FAPAR brought the highest output uncertainty on annual GPP. The output uncertainty, quantified as the standard deviation of the 500 simulations for each variable, was highest for FAPAR (79.9 gC m^{-2} $year^{-1}$) followed by VPD (55.2 gC m^{-2} $year^{-1}$) and incoming PAR (42.8 gC m^{-2} $year^{-1}$). The simultaneous effect of the included uncertainties generated an output standard deviation of 112 gC m^{-2} $year^{-1}$ for MOD17A2 NCEP II GPP. This corresponds to a 95% confidence interval of ±219 gC m^{-2} $year^{-1}$ for SD-DEM.

3.4. Light use efficiency

The ε_{max} values in the BPLUT used in the calculation of ε in the MOD17A2 algorithm for the two main ecosystem types are 1.21 gC MJ^{-1} for savannas and 0.86 gC MJ^{-1} for grasslands (Zhao & Running, 2010). Linear regressions with no offset were fitted to eddy covariance GPP and products of MOD17A2 FAPAR and tower PAR, VPD_s and T_s to determine an inferred ε_{max} for each ecosystem type (Fig. 8) and site (Table 3). For savannas, site variations in ε_{max} was high as it varied from 0.33 gC MJ^{-1} for ZA-MAP to 3.50 gC MJ^{-1} for ML-KEM (Table 3). The explained variance for savannas was low for both the inferred ε_{max} of 1.66 gC MJ^{-1} (36%) and the MOD17A2 ε_{max} of 1.21 gC MJ^{-1} (26%) (Fig. 8a). For grasslands a significant improvement was made with an ε_{max} of 2.01 gC MJ^{-1} which explained 74% of the variance in eddy covariance GPP whereas the ε_{max} of 0.86 gC MJ^{-1} used in MOD17A2 only explained 25% of the variance (Fig. 8b). For grasslands inferred ε_{max} varied between 1.58 gC MJ^{-1} (NE-WAM) to 2.92 gC MJ^{-1} (NE-WAF). Out of the 12 savanna and grassland sites, 10 had higher inferred ε_{max} compared to the MOD17A2 values for savanna and grassland biomes (Table 3).

4. Discussion

The MOD17A2 product has previously been evaluated for several biomes with a rather strong focus on northern latitude ecosystems (Coops et al., 2007; Heinsch et al., 2006; Sims et al., 2006; Turner et al., 2005, 2006; Xiao et al., 2004). Few studies have validated the product for savanna ecosystems (Fensholt et al., 2006; Kanniah et al., 2009; Leuning et al., 2005; Sjöström et al., 2011). In this study we used eddy covariance data for twelve African sites covering a total of thirty-one site years. Site mean differences between MOD17A2 and eddy covariance GPP were found to vary (Table 2), but a rather large underestimation was observed specifically for dry sites located in the Sahel.

There are uncertainties associated with the eddy covariance method (Loescher et al., 2006). Estimation on the uncertainty of eddy covariance based estimates of GPP is complex (Richardson et al., 2012) and may range from 10 to at least 50 gC m^{-1} $year^{-1}$ for NEE (Aubinet et al., 2000; Baldocchi, 2003). The GPP data in this study was obtained from NEE and R_{eco}, where R_{eco} was extrapolated by driving the relationship between nighttime R_{eco} and air temperature on day time air temperature as determined by Lloyd and Taylor (1994). Archibald et al. (2009) demonstrated that flux partioning at ZA-KRU could be improved by using more appropriate temperature functions at the site and by including controls from soil moisture. Merbold et al. (2009) further showed that temperature had an influence on R_{eco} for several of the sites included in this study. For the dry sites (<1000 mm of annual rainfall), however, R_{eco} was found to also be dependent on soil moisture. The standard methods used in the processing of the eddy covariance data might not always be appropriate for tropical ecosystems (Archibald et al., 2009). It should therefore be noted that the uncertainties associated with the flux partioning and the harsh temperature conditions found at many of the sites may result in undetermined biases.

Further uncertainties also arise due to scale mismatch between the eddy covariance footprint and the MODIS data. (Tan et al., 2006), for instance, reported that gridding artifacts together with effects of viewing geometry resulted in an average overlap of less than 30% between MODIS grid cells and actual observations. This makes direct comparison of field measurements with MODIS data problematic, as retrievals are not necessarily centered on the precise location of the pixel used. This problem may become less severe for homogenous landscapes (Tan et al., 2006).

Analysis of the NCEP-DOE II meteorological data drivers (T_{min}, VPD and PAR) used in the MODIS GPP algorithm showed some noticeable differences when compared to tower climate data. The NCEP-DOE II data are originally produced at a coarse resolution (Kanamitsu et al., 2002). These data are then further interpolated to a 1×1 km grid which is used by MOD17 to calculate GPP and NPP (Zhao et al., 2005). The initial coarse spatial resolution data has been shown to include biases (Betts et al., 2006; Zhao et al., 2006). Globally, interannual

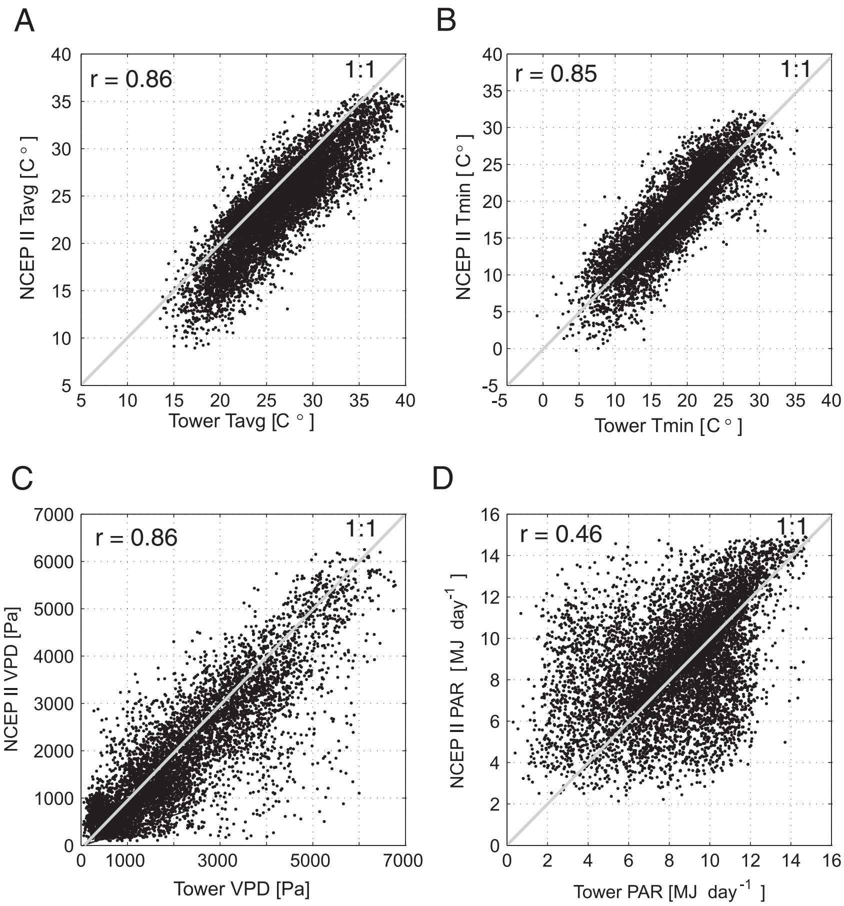

Fig. 5. Scatter plots showing daily NCEP-DOE II meteorology against daily tower meteorological data for T_{avg} (A), T_{min} (B), VPD (C) and PAR (D).

variability of NCEP-DOE II temperature have been shown to be similar to the CRUTEM3 dataset, which is based on instrumental observations (Zhao & Running, 2010). NCEP-DOE II T_{avg} was found to be underestimated (Fig. 5A). The slight underestimation in NCEP-DOE II VPD (Fig. 5C) could have been caused by uncertainties in T_{avg} as relatively small errors in temperature can introduce errors in VPD (Zhao et al., 2006). Radiation from reanalysis data generally contains large uncertainties (Kalnay et al., 1996), specifically in areas with a high spatial and temporal variability in cloud cover. Comparing incoming PAR from NCEP/DOE II versus field measured incoming PAR (Fig. 5D) showed a large amount of scatter that can influence the uncertainty of GPP estimated by MOD17 particularly during the growing seasons. This is, to a certain degree, reflected in the increased errors observed between MODIS NCEP II GPP and eddy covariance calculated GPP when only growing season points were included, but is also reflected in the increased correlations that were observed when driving MODIS GPP with tower data (data not shown). Alternative methods of deriving PAR, such as those presented by Liang et al. (2006) or Van Laake and Sanchez-Azofeifa (2005), both of which have been successfully applied on MODIS imagery, may increase the accuracy by which PAR is retrieved for large areas. However, none of these methods have yet been tested or implemented for MODIS at the global scale (Liang et al., 2010).

Replacing NCEP-DOE II with tower data in the MODIS GPP algorithm increased the correlation with eddy covariance GPP (Fig. 4B). Even though the overall correlation increased, larger underestimations were observed for many site-years. This effect has also previously been observed by Heinsch et al. (2006). When calibrating MOD17A2 at the global scale, the values in the BPLUT are influenced by observed biases in the global meteorological reanalysis dataset. For NCEP/DOE II, $S_{\downarrow}$ is globally overestimated whereas VPD is underestimated (Zhao et al., 2006). Thus, to get expected average annual GPP and NPP for given biome type's, parameter settings in the MOD17A2 BPLUT are used to counteract global under- or overestimations by NCEP/DOE II.

The comparison between VPD and GPP revealed that the VPD constraint on GPP is reasonable for grasslands (Fig. 6B). The overall pattern for savannas was less clear with especially one site (ML-KEM) showing strong assimilation even at high VPD (Fig. 6A). This is due to the nature of the site, which is inundated during the rain season and the beginning of the dry season. During this period, the site behaves like an irrigated site in a dry environment (Timouk et al., 2009). Access to water from the deeper soil layers for the trees may further explain the rather unclear pattern observed between VPD and GPP at savannas (Leuning et al., 2005). Merbold et al. (2009) reported a strong decrease in assimilation rates with increasing VPD above 2000 Pa whereas Kanniah, Beringer, and Hutley (2011) showed that VPD and GPP was strongly correlated along the Northern Australian Tropical Transect. In contrast, Garbulsky et al. (2010) reported a weak influence of VPD on ε for savannas. Daytime VPD is used in MODIS GPP to quantify water stress, whereas soil moisture availability, as previously proposed to be included in the algorithm by Leuning et al. (2005), is not implemented. A more shallow rooting depth for grasses compared to trees could explain why VPD can be used as a reasonable single constraint in grasslands but not in savannas as trees in savannas can have access to water even at times when the upper parts of the soil profile are characterized by limited water availability (Ardö et al., 2008; Otieno et al., 2005; Raddad & Luukkanen, 2007). In addition to

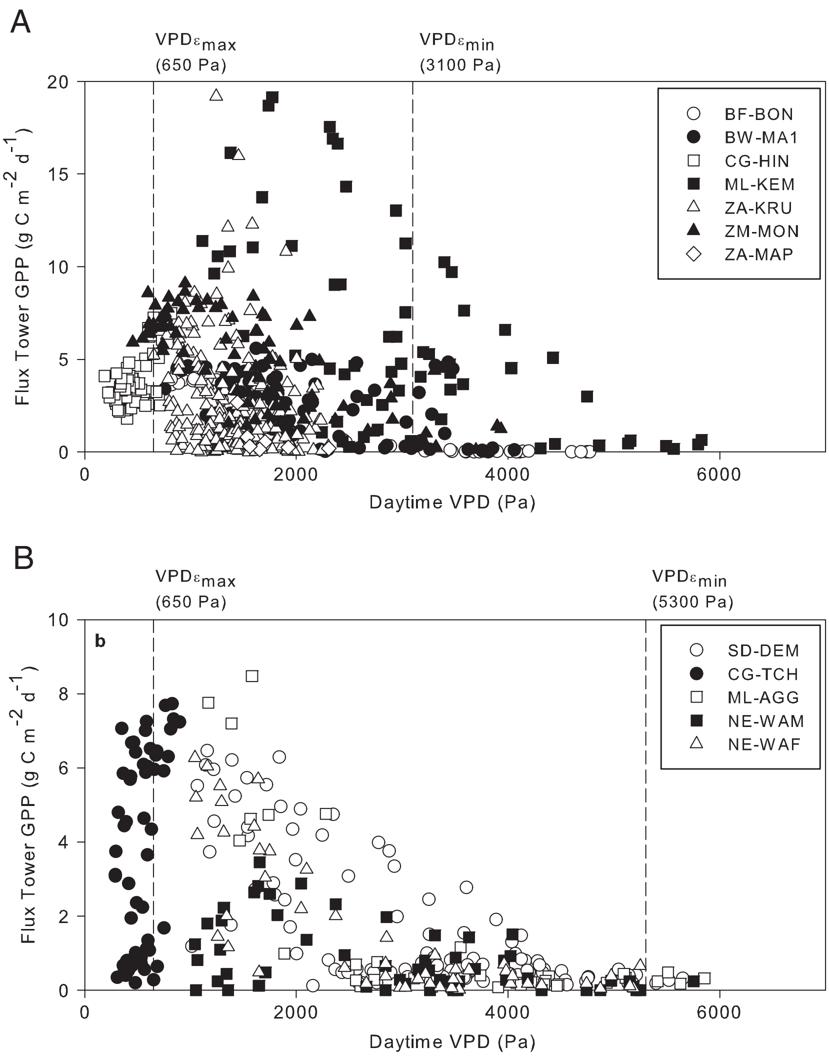

Fig. 6. 8-day eddy covariance estimated GPP (g Cm^{-2} day^{-1}) against 8-day average daytime tower VPD (Pa) for savannas (A) and grasslands (B). The dashed vertical lines mark the thresholds at which VPD inhibits photosynthesis in MOD17A2. VPD$_{\varepsilon max}$ is the daily average VPD at which ε is maximum (VPD scalar = 1) whereas VPD$_{\varepsilon min}$ is the daily average VPD at which ε is minimum (VPD scalar = 0).

the run-on effect at ML-KEM this may explain some of the scatter observed for savannas in Fig. 6A.

Comparisons of FAPAR calculated from field measurements with MOD15A2 FAPAR in savanna ecosystems has previously been presented for semi-arid Senegal (collection 4, Fensholt et al., 2004) and the Kalahari woodlands (collection 3, Huemmrich et al., 2005). Both of these studies revealed that the seasonal variation was captured well by the MODIS FAPAR product, however, FAPAR from MODIS was observed to be overestimated. Kanniah et al. (2009) found reasonable levels of MOD15A2 FAPAR as compared to field data which may indicate that the problem of FAPAR overestimation for savannas has been resolved in MOD15A2 collection 5. Although field calculated FAPAR-values in this study were observed to be slightly lower than MOD15A2 during the dry season (Fig. 7A) at the site in the Sudan, the major deviations occurred mainly at the start of the 2009 growing season. MODIS GPP uses a simple linear fitting to fill unreliable or missing MOD15A2 FAPAR (Zhao et al., 2005). Consecutive unreliable FAPAR values are linearly interpolated from the nearest reliable value prior and after it. Thus, the quality of the interpolation is determined by the accuracy of the FAPAR flagged as reliable. The linear interpolation across observations produced constant FAPAR which failed to match the green up observed in the FAPAR calculated from field data (Fig. 7A). In regions where the interference of clouds and aerosols is persistent during the growing season fitting functions such as those proposed by Jönsson and Eklundh (2004) may provide more realistically interpolated FAPAR time series than what is currently used in the MOD17A2 algorithm. However, by replacing the FAPAR used in MODIS Tower GPP with in situ calculated FAPAR it was shown that the rather large underestimation previously observed between eddy covariance GPP and MOD17A2 GPP during the peak vegetation season still remained (Fig. 7B). Thus, even though correct magnitudes of FAPAR would be provided, GPP would still be underestimated at SD-DEM in 2009.

Consideration must also be taken into the propagation of error in MODIS land cover into MOD15A2 FAPAR and MODIS GPP. MOD15A2 FAPAR is retrieved using a canopy radiation transfer model which requires MODIS land cover to define canopy structure type (Myneni et al., 2002). If a forest pixel, for instance, is incorrectly defined as grassland in MODIS land cover MOD15A2 FAPAR will be underestimated because the wrong canopy structure is used. Similarly, MODIS GPP will use the wrong ε_{max} in the BPLUT to calculate GPP.

Among the 12 sites included in this study, inferred site-specific ε_{max} from tower data and MOD17A2 FAPAR ranged from 0.33 to 3.50 gC MJ^{-1} (Table 3). Out of 12 sites, 10 had higher inferred ε_{max} compared to the MOD17A2 BPLUT values for savanna and grassland biomes and for 6 sites tower based ε_{max} values were more than twice the

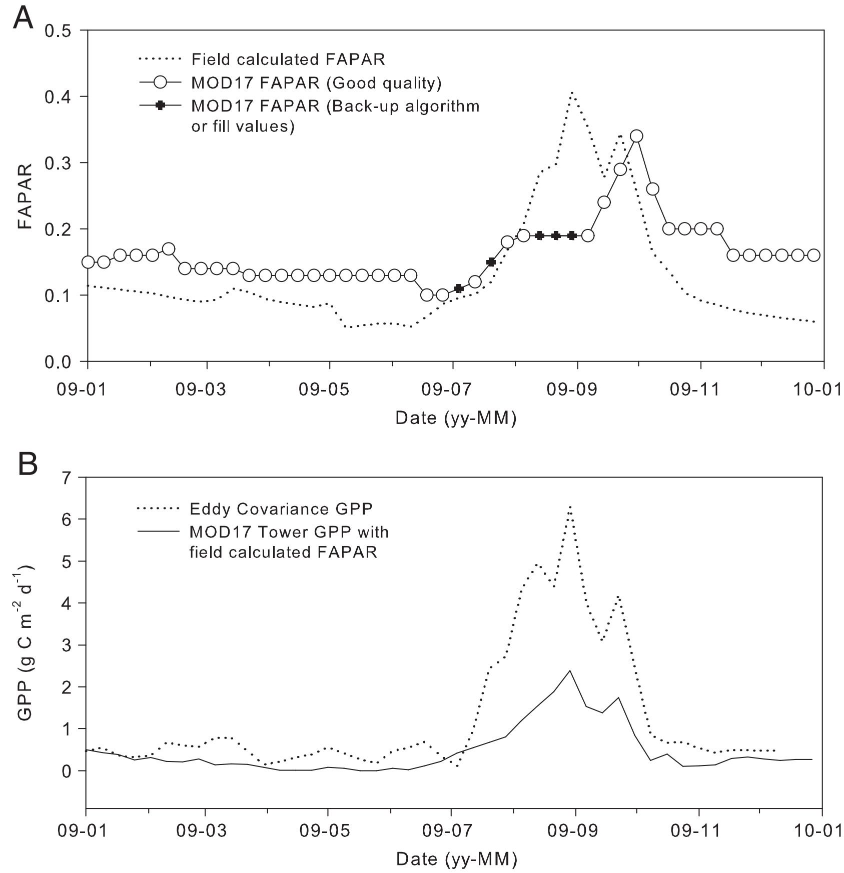

Fig. 7. Time-series of 8-day FAPAR from MOD17 against field calculated FAPAR (A). Crosses denote data points flagged as fill values by MOD15A2 (FparLai_QC, bit value 0). Bottom figure (b) shows eddy covariance estimated GPP (g Cm^{-2} day^{-1}) against GPP estimated by MOD17A2 using tower data and field calculated FAPAR (g Cm^{-2} day^{-1}) (B). Data is from 2009 for the site SD-DEM.

ε_{max} used in the MOD17A2 BPLUT. In addition to the uncertainties in the driver data, these differences may explain the underestimations observed in the comparisons between MODIS GPP and eddy covariance GPP at dry sites. Care must, however, be taken in the absolute interpretation of these results as underestimated MOD17A2 FAPAR (as observed at SD-DEM in 2009, Fig. 7) will lead to overestimated ε_{max}.

Recent studies have shown that ε_{max} can vary considerably both within and between vegetation types in response to environmental variation (Garbulsky et al., 2010; Sims et al., 2006; Wu et al., 2010). This variability may be hard to describe with a broad class (UMD) land cover dependent static ε_{max}, especially for savannas (Fig. 8a), and without consideration of soil moisture in dry areas (Gebremichael & Barros, 2006; Leuning et al., 2005). For grasslands, ε_{max} from the BPLUT is representative for grasslands globally (Heinsch et al., 2003) including different moisture regimes as well as varying proportions of C3/C4 grass (Merbold et al., 2009), factors that can influenced inferred ε_{max} (Fig. 8b). Garbulsky et al. (2010) reported average annual ε ranging from 0.34 to 2.01 g C MJ^{-1} for a range of vegetation types. Garbulsky et al. (2010) further stress that annual precipitation is more important than vegetation type in determining both average ε and ε_{max} in global comparisons. In addition, several existing LUE models have used ε_{max} above the ones found in the BPLUT of MOD17A2 for savannas and grasslands (e.g. Kanniah et al., 2009; Nouvellon et al., 2001; Seaquist, Olsson, & Ardö, 2003; Yuan et al., 2007).

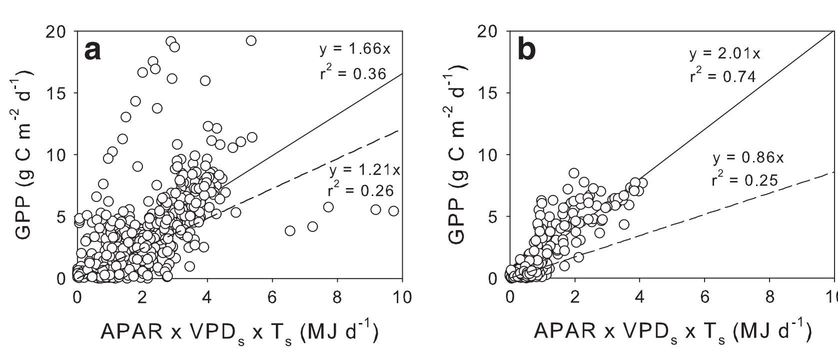

Fig. 8. 8-day eddy covariance estimated GPP (g Cm^{-2} day^{-1}) against the product of MOD17A2 FAPAR, tower PAR, VPD_s and T_s for savannas (a) and grasslands (b). Solid lines represent linear regression-estimated inferred ε_{max} whereas dashed lines represent the ε_{max} used by MOD17A2.

Table 3
Linear regression statistics (slope and coefficient of determination) for both inferred $\varepsilon_{max.}$ and MOD17A2 $\varepsilon_{max.}$ (no offset).

Site	Inferred ε_{max} (b_0, g CMJ^{-1})	R^2 (inferred ε_{max})	MOD17A2 ε_{max}	R^2 (MOD17A2 ε_{max})
SD-DEM	2.35	0.74	0.84	0.12
BF-BON	2.48	0.92	1.21	0.49
BW-MA	1.58	0.40	1.21	0.26
CG-HIN	1.77	0.55	1.21	–
CG-TCH	1.85	0.86	1.21	0.15
ML-AGG	2.16	0.65	0.86	0.28
ML-KEM	3.50	0.35	0.86	–
ZA-KRU	1.21	0.45	1.21	0.45
ZM-MON	1.87	0.79	1.21	0.22
ZA-MAP	0.33	0.32	1.21	–
NG-WAM	1.58	0.44	0.86	0.08
NG-WAF	2.92	0.56	0.86	–

5. Conclusion

In this study we evaluated the MOD17A2 GPP product through comparison with in situ measurements of meteorology and GPP for 12 African eddy covariance flux towers. MOD17A2 underestimated GPP with a mean difference of 0.70 gC m^{-2} day^{-1} but with considerable variability among the 31 site-years of data available. Seasonality was captured well but GPP was underestimated by MOD17A2 specifically for many of the dry sites. Differences in the driver data were found when comparing daily NCEP/DOE II and in situ observations. Replacing the NCEP/DOE II driver data (T_{min}, VPD, and incoming PAR) with tower measured data moderately improved the correlation with eddy covariance GPP. Inferred ε_{max} was significantly higher than the prescribed MOD17A2 ε_{max}. This in addition to uncertainties in FAPAR may explain the underestimations at dry sites. The results suggest that improved quality of driver data and FAPAR and a readjustment of the parameters in the BPLUT (primarily ε_{max}), may be needed to better estimate GPP for African ecosystems in MOD17A2. Additional in situ measurements of GPP and FAPAR are needed for a wider range of ecosystem types in Africa to allow for more systematic evaluations of MODIS GPP and its MODIS and non-MODIS inputs in African environments.

Acknowledgments

Financial support was provided by the Swedish National Space Board (contracts 120/06 and 74/08), the Swedish Research Council (VR 621–2004) and through the EU-funded CARBOAFRICA project (contract 037137). The Wankama stations in Niger are part of the French-funded AMMA-CATCH observatory (amma-catch.org), a component of the AMMA international program (amma-international.org). We would also like to thank the anonymous reviewers for their helpful comments.

Appendix A. Supplementary data

Supplementary data associated with this article can be found in the online version, at http://dx.doi.org/10.1016/j.rse.2012.12.023. These data include Google maps of the most important areas described in this article.

References

Archibald, S. A., Kirton, A., van der Merwe, M. R., Scholes, R. J., Williams, C. A., & Hanan, N. (2009). Drivers of inter-annual variability in Net Ecosystem Exchange in a semi-arid savanna ecosystem, South Africa. *Biogeosciences*, *6*, 251–266.

Ardö, J., Mölder, M., El-Tahir, B., & Elkhidir, H. (2008). Seasonal variation of carbon fluxes in a sparse savanna in semi arid Sudan. *Carbon Balance and Management*, *3*, 7.

Aubinet, M., Grelle, G., Ibrom, A., Rannik, U., Moncrieff, J., Foken, T., et al. (2000). Estimates of the annual net carbon and water exchange of European forests: The EUROFLUX methodology. *Advances in Ecological Research*, *30*, 113–175.

Baldocchi, D. D. (2003). Assessing the eddy covariance technique for evaluating carbon dioxide exchange rates of ecosystems: Past, present and future. *Global Change Biology*, *9*, 479–492.

Baldocchi, D., Falge, E., Lianhong, G., Olson, R., Hollinger, D., Running, S., et al. (2001). FLUXNET: A new tool to study the temporal and spatial variability of ecosystem-scale carbon dioxide, water vapor, and energy flux densities. *Bulletin of the American Meteorological Society*, *82*, 2415.

Betts, A. K., Zhao, M., Dirmeyer, P. A., & Beljaars, A. C. M. (2006). Comparison of ERA40 and NCEP/DOE near-surface data sets with other ISLSCP-II data sets. *Journal of Geophysical Research*, *111*, D22S04.

Bombelli, A., Henry, M., Castaldi, S., Adu-Bredu, S., Arneth, A., de Grandcourt, A., et al. (2009). An outlook on the Sub-Saharan Africa carbon balance. *Biogeosciences*, *6*, 2193–2205.

Boulain, N., Cappelaere, B., Ramier, D., Issoufou, H. B. A., Halilou, O., Seghieri, J., et al. (2009). Towards an understanding of coupled physical and biological processes in the cultivated Sahel — 2. Vegetation and carbon dynamics. *Journal of Hydrology*, *375*, 190–203.

Brummer, C., Falk, U., Papen, H., Szarzynski, J., Wassmann, R., & Bruggemann, N. (2008). Diurnal, seasonal, and interannual variation in carbon dioxide and energy exchange in shrub savanna in Burkina Faso (West Africa). *Journal of Geophysical Research*, *113*.

Connolly, J., Roulet, N. T., Seaquist, J. W., Holden, N. M., Lafleur, P. M., Humphreys, E. R., et al. (2009). Using MODIS derived fPAR with ground based flux tower measurements to derive the light use efficiency for two Canadian peatlands. *Biogeosciences*, *6*, 225–234.

Coops, N. C., Black, T. A., Jassal, R. P. S., Trofymow, J. A. T., & Morgenstern, K. (2007). Comparison of MODIS, eddy covariance determined and physiologically modelled gross primary production (GPP) in a Douglas-fir forest stand. *Remote Sensing of Environment*, *107*, 385–401.

Coops, N. C., Jassal, R. S., Leuning, R., Black, A. T., & Morgenstern, K. (2007). Incorporation of a soil water modifier into MODIS predictions of temperate Douglas-fir gross primary productivity: Initial model development. *Agricultural and Forest Meteorology*, *147*, 99–109.

Fensholt, R., Sandholt, I., & Rasmussen, M. S. (2004). Evaluation of MODIS LAI, fAPAR and the relation between fAPAR and NDVI in a semi-arid environment using in situ measurements. *Remote Sensing of Environment*, *91*, 490–507.

Fensholt, R., Sandholt, I., Rasmussen, M. S., Stisen, S., & Diouf, A. (2006). Evaluation of satellite based primary production modelling in the semi-arid Sahel. *Remote Sensing of Environment*, *105*, 173–188.

Garbulsky, M. F., Penuelas, J., Papale, D., Ardö, J., Goulden Michael, L., Kiely, G., et al. (2010). Patterns and controls of the variability of radiation use efficiency and primary productivity across terrestrial ecosystems. *Global Ecology and Biogeography*, *19*, 253–267.

Gebremichael, M., & Barros, A. P. (2006). Evaluation of MODIS gross primary productivity (GPP) in tropical monsoon regions. *Remote Sensing of Environment*, *100*, 150–166.

Heinsch, F. A., Reeeves, M., Votava, P., Kang, S., Milesi, C., Zhao, M., et al. (2003). Users guide GPP and NPP (MOD17A2/A3) products. NASA MODIS land algorithm (version 2.0.). University of Montana, NTSG.

Heinsch, F. A., Zhao, M., Running, S. W., Kimball, J. S., Nemani, R. R., Davis, K. J., et al. (2006). Evaluation of remote sensing based terrestrial productivity from MODIS using regional tower eddy flux network observations. *IEEE Transactions on Geoscience and Remote Sensing*, *44*, 1908–1925.

Huemmrich, K. F., Privette, J. L., Mukelabai, M., Myneni, R. B., & Knyazikhin, Y. (2005). Time-series validation of MODIS land biophysical products in a Kalahari woodland, Africa. *International Journal of Remote Sensing*, *26*, 4381–4398.

Hulme, M., Doherty, R., Ngara, T., New, M., & Lister, D. (2001). African climate change: 1900–2100. *Climate Research*, *17*, 145–168.

Jönsson, P., & Eklundh, L. (2004). TIMESAT — A program for analyzing time-series of satellite sensor data. *Computers and Geosciences*, *30*, 833–845.

Kalnay, E., Kanamitsu, M., Kistler, R., Collins, W., Deaven, D., Gandin, L., et al. (1996). The NCEP/NCAR 40-year reanalysis project. *Bulletin of the American Meteorological Society*, *77*, 437–471.

Kanamitsu, M., Ebisuzaki, W., Woollen, J., Yang, S. -K., Hnilo, J. J., Fiorino, M., et al. (2002). NCEP-DOE AMIP-II reanalysis (R-2). *Bulletin of the American Meteorological Society*, *83*, 1631–1643.

Kanniah, K. D., Beringer, J., & Hutley, L. B. (2011). Environmental controls on the spatial variability of savanna productivity in the Northern Territory, Australia. *Agricultural and Forest Meteorology*, *151*, 1429–1439.

Kanniah, K. D., Beringer, J., Hutley, L. B., Tapper, N. J., & Zhu, X. (2009). Evaluation of collections 4 and 5 of the MODIS Gross Primary Productivity product and algorithm improvement at a tropical savanna site in northern Australia. *Remote Sensing of Environment*, *113*, 1808–1822.

Kutsch, W. L., Hanan, N., Scholes, B., McHugh, I., Kubheka, W., Eckhardt, H., et al. (2008). Response of carbon fluxes to water relations in a savanna ecosystem in South Africa. *Biogeosciences*, *5*, 1797–1808.

Lebel, T., Cappelaere, B., Galle, S., Hanan, N., Kergoat, L., Levis, S., et al. (2009). AMMA-CATCH studies in the Sahelian region of West-Africa: An overview. *Journal of Hydrology*, *375*, 3–13.

Leuning, R., Cleugh, H. A., Zegelin, S. J., & Hughes, D. (2005). Carbon and water fluxes over a temperate Eucalyptus forest and a tropical wet/dry savanna in Australia: Measurements and comparison with MODIS remote sensing estimates. *Agricultural and Forest Meteorology*, *129*, 151–173.

Liang, S. L., Wang, K. C., Zhang, X. T., & Wild, M. (2010). Review on estimation of land surface radiation and energy budgets from ground measurement, remote sensing and model simulations. *IEEE Journal of Selected Topics in Applied Earth Observations and Remote Sensing*, *3*, 225–240.

Liang, S. L., Zheng, T., Liu, R. G., Fang, H. L., Tsay, S. C., & Running, S. (2006). Estimation of incident photosynthetically active radiation from Moderate Resolution Imaging Spectrometer data. *Journal of Geophysical Research*, *111*, D15208.

Lindroth, A., Grelle, A., & Moren, A. S. (1998). Long-term measurements of boreal forest carbon balance reveal large temperature sensitivity. *Global Change Biology*, *4*, 443–450.

Lloyd, J., & Taylor, J. (1994). On the temperature dependence of soil respiration. *Functional Ecology*, *8*, 315–323.

Loescher, H. W., Law, B. E., Mahrt, L., Hollinger, D. Y., Campbell, J., & Wofsy, S. C. (2006). Uncertainties in, and interpretation of, carbon flux estimates using the eddy covariance technique. *Journal of Geophysical Research-Atmospheres*, *111*, D21S90.

Longdoz, B., Granier, A., Loustau, D., Bakker, M., Delzon, S., Kowalski, A. S., et al. (2010). Environmental control of carbon fluxes in forest ecosystems in France: A comparison of temperate, Mediterranean and tropical forests. In D. Loustau (Ed.), *Forests, carbon cycle and climate change* (pp. 27–53). Paris: Quae editions.

Merbold, L., Ardö, J., Arneth, A., Scholes, R. J., Nouvellon, Y., de Grandcourt, A., et al. (2009). Precipitation as driver of carbon fluxes in 11 African ecosystems. *Biogeosciences*, *6*, 1027–1041.

Monteith, J. L. (1977). Climate and the efficiency of crop production in Britain. *Philosophical Transactions of the Royal Society of London. Series B, Biological Sciences*, *281*, 277–294.

Montieth, J. L. (1972). Solar radiation and productivity in tropical ecosystems. *Journal of Applied Ecology*, *9*, 747–766.

Myneni, R. B., Hoffman, S., Knyazikhin, Y., Privette, J. L., Glassy, J., Tian, Y., et al. (2002). Global products of vegetation leaf area and fraction absorbed PAR from year one of MODIS data. *Remote Sensing of Environment*, *83*, 214–231.

Nicholson, S. E. (2000). The nature of rainfall variability over Africa on time scales of decades to millennia. *Global and Planetary Change*, *26*, 137–158.

Nicholson, S. E. (2001). Climatic and environmental change in Africa during the last two centuries. *Climate Research*, *17*, 123–144.

Nouvellon, Y., Moran, M. S., Lo Seen, D., Bryant, R., Rambal, S., Ni, W. M., et al. (2001). Coupling a grassland ecosystem model with Landsat imagery for a 10-year simulation of carbon and water budgets. *Remote Sensing of Environment*, *78*, 131–149.

Otieno, D., Schmidt, M., Kinyamario, J., & Tenhunen, J. (2005). Responses of *Acacia tortilis* and *Acacia xanthophloea* to seasonal changes in soil water availability in the savanna region of Kenya. *Journal of Arid Environments*, *62*, 377–400.

Papale, D., Reichstein, M., Aubinet, M., Canfora, E., Bernhofer, C., Kutsch, W., et al. (2006). Towards a standardized processing of Net Ecosystem Exchange measured with eddy covariance technique: algorithms and uncertainty estimation. *Biogeosciences*, *3*, 571–583.

Papale, D., & Valentini, R. (2003). A new assessment of European forests carbon exchanges by eddy fluxes and artificial neural network spatialization. *Global Change Biology*, *9*, 525–535.

Parry, M. L., Canziani, O. F., Palutikof, J. P., van der Linden, P. J., & Hanson, C. E. (2007). *Climate change 2007: Impacts, adaptation and vulnerability. Contribution of working group I to the fourth assessment report of the Intergovernmental Panel on Climate Change.* Cambridge: Cambridge University Press.

Plummer, S. (2006). On validation of the MODIS gross primary production product. *IEEE Transactions on Geoscience and Remote Sensing*, *44*, 1936–1938.

Raddad, E., & Luukkanen, O. (2007). The influence of different *Acacia senegal* agroforestry systems on soil water and crop yields in clay soils of the Blue Nile region, Sudan. *Agricultural Water Management*, *87*, 61–72.

Ramier, D., Boulain, N., Cappelaere, B., Timouk, F., Rabanit, M., Lloyd, C. R., et al. (2009). Towards an understanding of coupled physical and biological processes in the cultivated Sahel — 1. Energy and water. *Journal of Hydrology*, *375*, 204–216.

Reichstein, M., Falge, E., Baldocchi, D., Papale, D., Aubinet, M., Berbigier, P., et al. (2005). On the separation of net ecosystem exchange into assimilation and ecosystem respiration: Review and improved algorithm. *Global Change Biology*, *11*, 1424–1439.

Richardson, A. D., Aubinet, M., Barr, A. G., Hollinger, D. Y., Ibrom, A., Lasslop, G., et al. (2012). Uncertainty quantification. In M. Aubinet, T. Vesala, & D. Papale (Eds.), *Eddy covariance: A practical guide to measurement and data analysis* (pp. 173–209). Netherlands: Springer.

Richmond, A., Kaufmann, R. K., & Myneni, R. B. (2007). Valuing ecosystem services: A shadow price for net primary production. *Ecological Economics*, *64*, 454–462.

Schlenker, W., & Lobell, D. B. (2010). Robust negative impacts of climate change on African agriculture. *Environmental Research Letters*, *5*, 8.

Schwalm, C. R., Williams, C. A., & Schaefer, K. (2011). Carbon consequences of global hydrologic change, 1948–2009. *Journal of Geophysical Research — Biogeosciences*, *116*, 7.

Seaquist, J. W., Olsson, L., & Ardö, J. (2003). A remote sensing-based primary production model for grassland biomes. *Ecological Modelling*, *169*, 131–155.

Sellers, P. J., Los, S. O., Tucker, C. J., Justice, C. O., Dazlich, D. A., Collatz, G. J., et al. (1996). A revised land surface parameterization (SiB2) for atmospheric GCMS. Part II: The generation of global fields of terrestrial biophysical parameters from satellite data. *Journal of Climate*, *9*, 706–737.

Sims, D. A., Rahman, A. F., Cordova, V. D., El-Masri, B. Z., Baldocchi, D. D., Flanagan, L. B., et al. (2006). On the use of MODIS EVI to assess gross primary productivity of North American ecosystems. *Journal of Geophysical Research*, *111*, G04015.

Sjöström, M., Ardö, J., Arneth, A., Boulain, N., Cappelaere, B., Eklundh, L., et al. (2011). Exploring the potential of MODIS EVI for modeling gross primary production across African ecosystems. *Remote Sensing of Environment*, *115*, 1081–1089.

Solomon, S. D., Qin, M., Manning, Z., Chen, M., Marquis, K. B., Averyt, M., et al. (2007). *The physical science basis. Contribution of working group I to the Fourth Assessment Report of the Intergovernmental Panel on Climate Change.* Cambridge, United Kingdom and New York, NY, USA.

Tan, B., Woodcock, C. E., Hu, J., Zhang, P., Ozdogan, M., Huang, D., et al. (2006). The impact of gridding artifacts on the local spatial properties of MODIS data: Implications for validation, compositing, and band-to-band registration across resolutions. *Remote Sensing of Environment*, *105*, 98–114.

Timouk, F., Kergoat, L., Mougin, E., Lloyd, C. R., Ceschia, E., Cohard, J. M., et al. (2009). Response of surface energy balance to water regime and vegetation development in a Sahelian landscape. *Journal of Hydrology*, *375*, 178–189.

Turner, D. P., Ritts, W. D., Cohen, W. B., Gower, S. T., Running, S. W., Zhao, M. S., et al. (2006). Evaluation of MODIS NPP and GPP products across multiple biomes. *Remote Sensing of Environment*, *102*, 282–292.

Turner, D. P., Ritts, W. D., Cohen, W. B., Gower, S. T., Zhao, M. S., Running, S. W., et al. (2003). Scaling gross primary production (GPP) over boreal and deciduous forest landscapes in support of MODIS GPP product validation. *Remote Sensing of Environment*, *88*, 256–270.

Turner, D. P., Ritts, W. D., Cohen, W. B., Maeirsperger, T. K., Gower, S. T., Kirschbaum, A. A., et al. (2005). Site-level evaluation of satellite-based global terrestrial gross primary production and net primary production monitoring. *Global Change Biology*, *11*, 666–684.

Van Laake, P. E., & Sanchez-Azofeifa, G. A. (2005). Mapping PAR using MODIS atmosphere products. *Remote Sensing of Environment*, *94*, 554–563.

Veenendaal, M. E., Kolle, O., & Lloyd, J. (2004). Seasonal variation in energy fluxes and carbon dioxide exchange for a broad leaved semi-arid savanna (Mopane woodland) in Southern Africa. *Global Change Biology*, *10*, 318–328.

Williams, C. A., Hanan, N. P., Baker, I., Collatz, G. J., Berry, J., & Denning, A. S. (2008). Interannual variability of photosynthesis across Africa and its attribution. *Journal of Geophysical Research*, *113*, G04015.

Williams, C., Hanan, N., Neff, J., Scholes, R., Berry, J., Denning, A. S., et al. (2007). Africa and the global carbon cycle. *Carbon Balance and Management*, *2*, 3.

Wofsy, S. C., Goulden, M. L., Munger, J. W., Fan, S. -M., Bakwin, P. S., Daube, B. C., et al. (1993). Net exchange of CO_2 in a mid-latitude forest. *Science*, *260*, 1314–1317.

Wu, C. Y., Munger, J. W., Niu, Z., & Kuang, D. (2010). Comparison of multiple models for estimating gross primary production using MODIS and eddy covariance data in Harvard Forest. *Remote Sensing of Environment*, *114*, 2925–2939.

Xiao, X. M., Zhang, Q. Y., Braswell, B., Urbanski, S., Boles, S., Wofsy, S., et al. (2004). Modeling gross primary production of temperate deciduous broadleaf forest using satellite images and climate data. *Remote Sensing of Environment*, *91*, 256–270.

Yuan, W., Liu, S., Zhou, G., Zhou, G., Tieszen, L. L., Baldocchi, D., et al. (2007). Deriving a light use efficiency model from eddy covariance flux data for predicting daily gross primary production across biomes. *Agricultural and Forest Meteorology*, *143*, 189–207.

Zhang, Q., Xiao, X., Braswell, B., Linder, E., Ollinger, S., Smith, M. -L., et al. (2006). Characterization of seasonal variation of forest canopy in a temperate deciduous broadleaf forest, using daily MODIS data. *Remote Sensing of Environment*, *105*, 189–203.

Zhao, M., Heinsch, F. A., Nemani, R. R., & Running, S. W. (2005). Improvements of the MODIS terrestrial gross and net primary production global data set. *Remote Sensing of Environment*, *95*, 164–176.

Zhao, M., & Running, S. W. (2010). Drought-induced reduction in global terrestrial net primary production from 2000 through 2009. *Science*, *329*, 940–943.

Zhao, M., Running, S. W., & Nemani, R. R. (2006). Sensitivity of Moderate Resolution Imaging Spectroradiometer (MODIS) terrestrial primary production to the accuracy of meteorological reanalyses. *Journal of Geophysical Research*, *111*, G01002.